

# The crack growth mechanism in asphaltic mixes

Maarten M.J. Jacobs  
Delft University of Technology

Piet C. Hopman and André A.A. Molenaar  
Delft University of Technology, Road and Railroad Research Laboratory

The crack growth mechanism in asphalt concrete (AC) mixes is studied. In cyclic tests on several asphaltic mixes crack growth is measured, both with crack foils and with COD-gauges. It is found that crack growth in asphaltic mixes is described by three processes which are parallel in time: cohesive crack growth in the mortar, adhesive crack growth between the mortar and the aggregates and a crack stoppers process. Differences in overall crack growth in asphalt concrete are due to differences in the contributions of each individual process to the overall process.

*Keywords:* asphalt concrete, fracture, PRINCALS analyses, micro crack zone, cohesive crack growth, adhesive crack growth, crack arresters, uniaxial tensile test, absolute rate theory.

## 1 Introduction

In The Netherlands crack growth was and is a very important damage in flexible pavements. About 60 percent of the yearly road maintenance budget (in 1991 about 2.5 billion Dutch guilders) is spent on the repair of this damage. In general two types of cracks occur in asphalt pavement structures: cracks which start at the bottom of the AC layer and grow upwards and cracks which are initiated at the surface and grow downwards (surface cracks). Given the effects cracking has on the durability of surface layers and so indirectly on the capacity of the road network (maintenance works), it is obvious that a study into cracking of asphalt mixes in general and of wearing courses in particular is justified.

The objective of the research was to acquire more insight into the crack growth and crack resistance characteristics of AC mixes. The practical aims were to advance insight into the influence of mix components and loading conditions on the fatigue and crack growth behaviour and to contribute to the understanding of the interactive behaviour of the mortar, the aggregates and the air voids. By this, the crack growth resistance of mixes could be improved in practice.

In this paper first attention is paid to the cyclic crack growth experiments by means of the uniaxial tensile test on several kinds of AC top layer mixes. The measurements are carried out in two ways: with a crack foil to measure the crack growth at the outside of the specimen and with Crack

Opening Displacement (COD) gauges to measure the fracture process in the specimen. Statistical analyses with the crack foil measurements as input show that during the crack propagation phase three parallel crack growth processes occur. Principal Components Analysis shows that the physical meaning of these three crack growth processes are: cohesive crack growth, adhesive crack growth and crack retardation. Comparing the crack foil and COD-measurements information is gained about the micro crack zone in front of the micro crack. With a different theoretical approach, based on the Absolute Rate Theory (ART), using the COD measurements as input for the determination of the ART-parameters, the same three parallel processes can be recognized. Both the analyses with the crack foil and COD-measurements as input will be discussed in this paper. A more comprehensive discussion is given by Jacobs (1995).

## 2 The experimental program

To obtain crack growth characteristics of AC mixes, an experimental program has been carried out by Jacobs (1995). A displacement controlled uniaxial tensile test has been used to ensure a stable crack growth phase. The specimens are loaded with a sinusoidal signal, both with and without rest periods. The dimensions of the specimens are 50 mm by 50 mm by 150 mm. Notched specimens are used to define the fracture zone in the specimen (see Fig. 1). Most of the tests are carried out at a loading frequency of 8 Hz. The measurements were carried out in a temperature controlled room where the temperature is set at 5, 15 and 25°C. The following quantities have been determined:

- (1) Resilient displacement, between the top and bottom loading plate.
- (2) Applied force (to achieve the required displacement).
- (3) Phase angle (between the load and displacement).
- (4) Macro crack length at the outside of the specimen, using crack foils. The foil is applied at one side of the specimen only. A ladder type foil is used with a rung distance of 1 mm and a rung length of 41 mm. The thickness of the foil is 5  $\mu\text{m}$  and the foil is incised before the start of the test reducing the crack growth resistance of the foil to a minimum. Therefore the influence of the foil on the crack growth process can be neglected. Each rung is connected to a channel of a multiprogrammer which detects every 2 seconds the state of the rung: broken or not. Thus the length of the macro crack at the outside of the specimen is obtained.
- (5) Crack Opening Displacement (COD). In both the notches of the specimen clip-gauges are fixed, which measure the resilient vertical deformation between the two horizontal planes in the notch. So information about the overall crack growth process in the area between the notches is obtained.
- (6) Number of load repetitions imposed on the specimen.

All measurements are done in triplicate at least.

To study the fatigue and crack growth process in AC mixes, a wide range of mixes were tested: sand asphalt (SA), dense asphalt concrete 0/8 (DAC8), dense asphalt concrete 0/16 (DAC16), dense asphalt concrete 0/16 with a modified binder (DACmod) and stone mastic asphalt 0/11 (SMA). Detailed information about the mixes is given by Jacobs (1995).

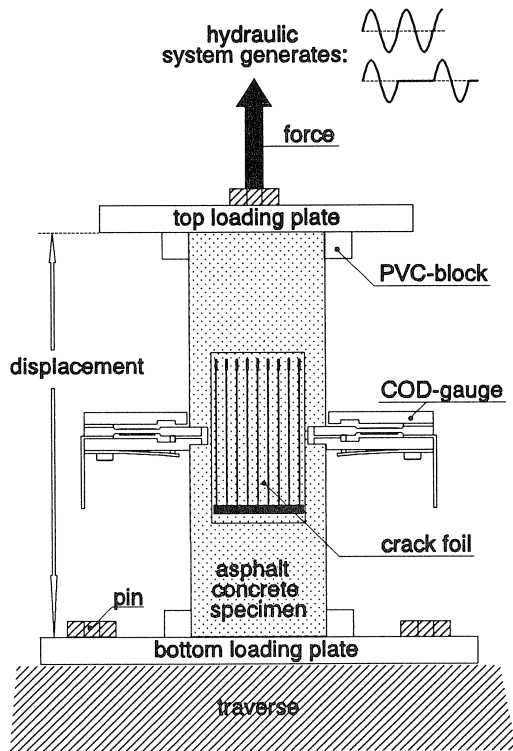


Fig. 1. Schematic overview of the specimen and the measurements.

The SA, DAC8, DACmod and SMA specimens are tested under various loading conditions: temperature (5, 15 and 25°C), frequency (2, 4, 8 and 16 Hz), deformation level (life span 0.5, 1, 2 and 4 hours) and kind of loading signal (sinusoidal, sinusoidal with rest periods, haversine). For the DAC16 mix only the test temperature is varied. For this latter mix variations in mix composition are introduced which occur in practice. The chosen variations are degree of compaction (96, 98 and 100%), percentage bitumen (5.7, 5.95, 6.2 and 6.7% m/m), percentage filler (5.5, 6.5 and 7.5% m/m) and type of aggregate (moraine, porphyry and granite).

In Fig. 2 an example of the measurements is given. On the right hand side of this figure, in the upper half, COD measurements at both sides of the specimen are shown. At the lower half the reduction of the cross section area, measured by the crack foil, are given. In the interpretation of the crack foil measurements it is assumed that the crack length is the distance of the broken rung to the side of the notch. The remaining cross section area is obtained by multiplying the difference between the width of the specimen (between the notches) and the crack length by the thickness. The main reason for using this interpretation is that in this way also the position of the crack in the specimen is indicated.

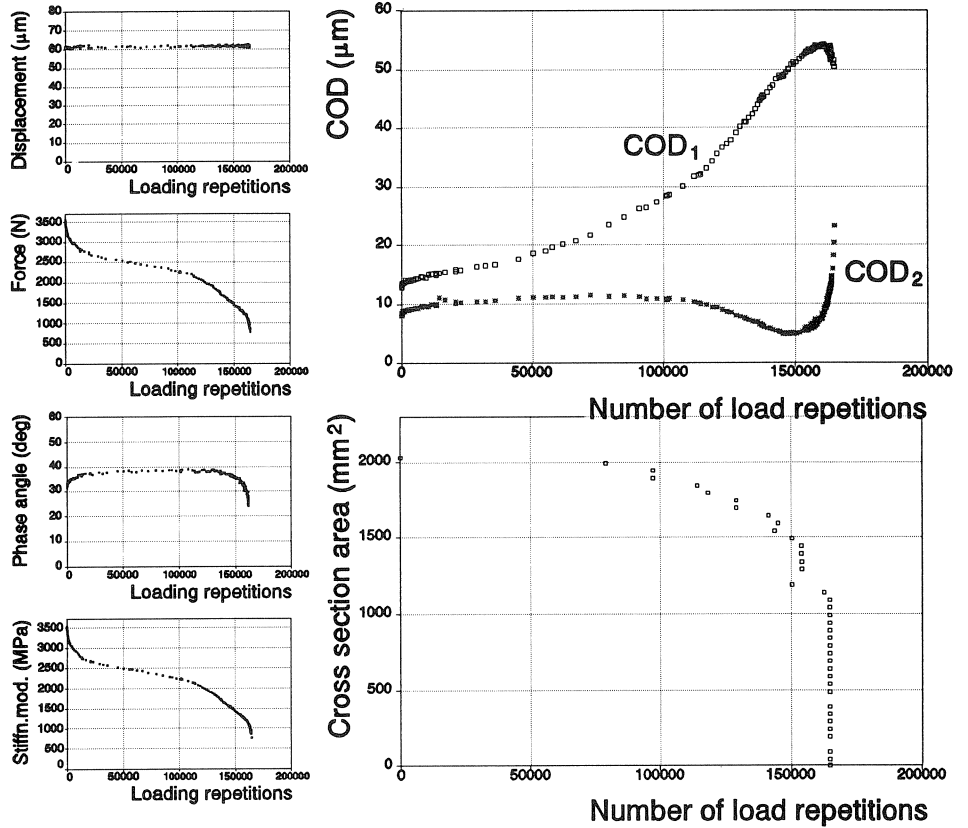


Fig. 2. Results of the crack growth measurements during a displacement controlled fatigue test (SA\_102, 15°C, 61  $\mu\text{m}$ , 2 Hz).

Analyzing the crack planes after cyclic fracture of the specimen (see Fig. 3), it may be observed that the crack growth process has three phenotypes:

- (1) a matt black crack surface, indicating crack growth through the mortar of the mix.
- (2) bare aggregate parts (without mortar) and by a gleaming black surface at the opposite plane, indicating crack growth between the aggregate and mortar along the surface of the aggregates.
- (3) places near aggregate parts, where the direction of crack propagation is changed due to the presence of the aggregate, thus indicating crack arrestors or crack retarders.

The actual crack growth is an addition of the three mechanisms yielding these phenotypes.

During an overall crack growth process their relative importance may vary: even one or the other may be absent. In the following paragraphs the description of the fracture process in AC mixes with three parallel phases will be verified, using the crack foil and COD measurements as input.

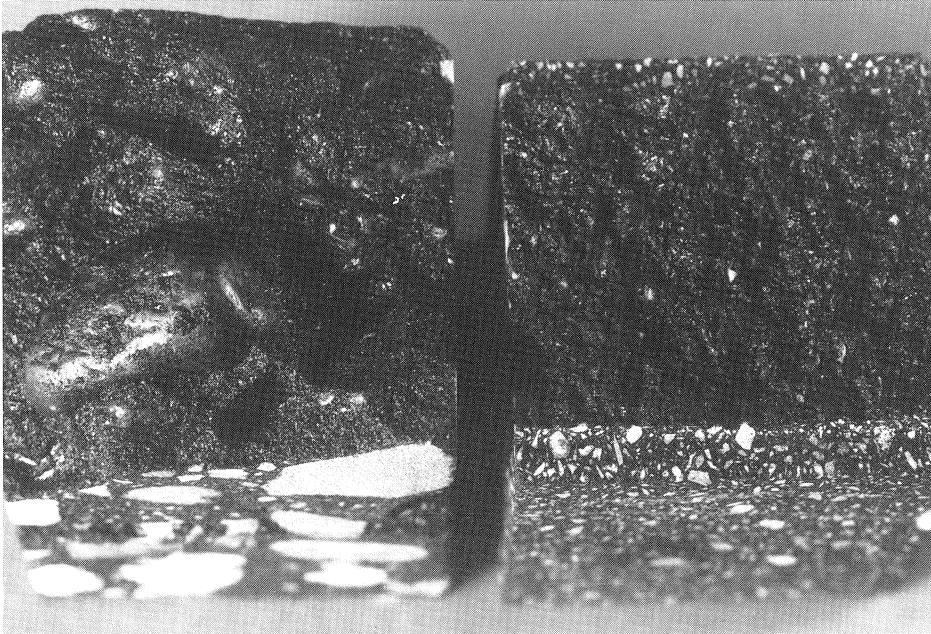


Fig. 3. A picture of the crack planes after dynamic failure of a SA (right) and a GAC specimen (left).

### 3 The crack foil measurements

Surveying the crack foil measurements, it is observed that:

- (1) the macro crack grows from one side of the specimen to the other and not from both sides to the middle. The asymmetric crack growth is in accordance with the results of calculations by Hordijk and Reinhardt (1989), who proved that the uniaxial tensile test in non-homogeneous materials (i.e. Portland cement concrete) is in fact a bending test. Non-uniform stress and strain distributions occur in the specimens due to differences in stiffness moduli between the components of the mix. This means that in all specimens a preferential side for crack growth exists. The growth of the macro crack from one to the other side is confirmed by the results of the COD-measurements: at the side where the macro crack starts the COD increases during the test ( $=COD_1$ ), while the other one ( $COD_2$ ) decreases,
- (2) the macro crack, measured by the crack foil, grows discontinuously. This is illustrated in Fig. 4, where the same crack foil interpretation is used as in Fig. 2. It seems that several small macro cracks occur in the specimen, which finally grow together into one large macro crack. It is even possible that crack growth is retarded because of the presence of aggregates in the area where the macro crack growth is measured. This retardation occurs primarily in mixes with larger aggregates, e.g. in DAC16 specimens.

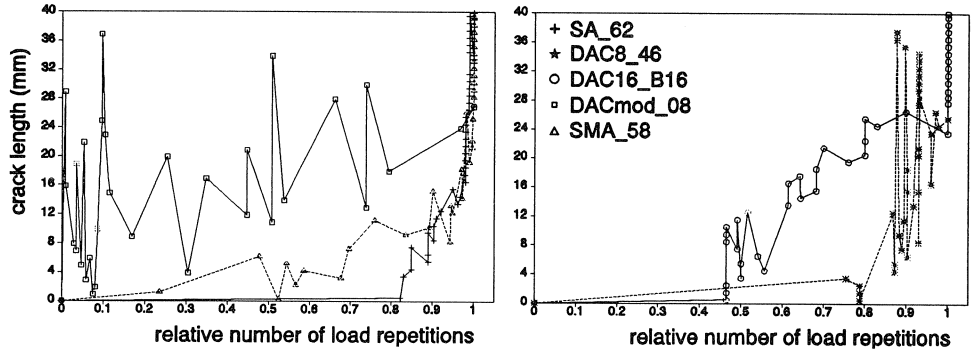


Fig. 4. Examples of the discontinuous crack growth process (crack foil interpretation).

All tests are analyzed in several terms (see Fig. 5):

- the number of load repetitions at which the first rung of the crack foil is broken (called crack initiation  $N_i$ ),
- the number of load repetitions until collapse of the specimen  $N_c$ ,
- the ratio  $N_{rel}$  between  $N_i$  and  $N_c$ ,
- the ratio  $S_{m,rel}$  between the stiffness modulus at crack initiation  $S_m(N_i)$  and the initial stiffness  $S_m(0)$  of the specimens.

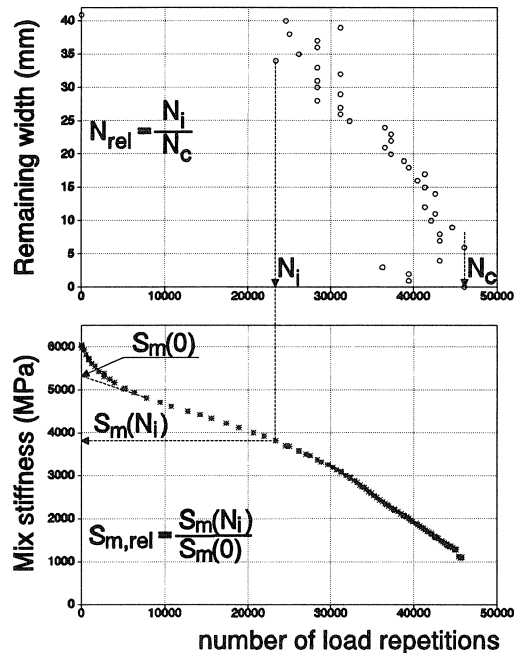


Fig. 5. Definition of crack growth parameters (specimen DAC16\_A35, 15°C).

$N_{rel}$  gives information about the crack growth speed whereas  $S_{m,rel}$  is an indicator for crack initiation. It is noted that a strong correlation exists between the type of mix on one hand and  $N_{rel}$  and  $S_{m,rel}$  on the other: the crack growth velocity increases with decreasing aggregate size (see Table 1) for the more traditional mixes SA, DAC8 and DAC16. This means that SA specimens break more brittle than DAC8 and DAC16 specimens. The SMA specimens show a very gradual crack growth process: an early crack initiation at a relative high stiffness modulus.

Although for some mixes the data in table 1 are based on relatively few measurements it is noted that the ratio between the initial stiffness modulus and the stiffness modulus at crack initiation decreases with increasing aggregate size, excluding SMA; in this latter mix crack growth starts already after a stiffness reduction of 22%. As the occurrence of cracks has a negative effect on the structural behaviour of a road structure, it is recommended to define the fatigue life in road design procedures as the number of load repetitions at which the stiffness modulus of the AC material has reduced to about 75% of its initial value instead of the nowadays used 50% reduction. This 75 percentage point is confirmed by the findings of Hopman et al.(1989).

Table 1. Mean ( $\mu$ ) and sample variation ( $\sigma_{n-1}$ ) of the crack growth velocity and crack indicator out of the crack foil measurements.

Mixcode	$N_i/N_c$		$S_m(N_i)/S_m(0)$	
	$\mu$	$\sigma_{n-1}$	$\mu$	$\sigma_{n-1}$
SA	0.68	0.11	0.76	0.10
DAC8	0.61	0.15	0.71	0.12
DAC16	0.59	0.13	0.69	0.08
SMA	0.40	0.19	0.78	0.13

To get a deeper understanding of the relationships between the variables, Principal Component Analyses (PCA) have been carried out on data from the crack foil measurements. PCA is a multivariate data reduction technique for analyzing relationships within a set of variables and is mainly used for two purposes: to identify groups of inter-correlated variables, and to reduce the number of variables being studied without losing essential information. In this study the PCA technique PRINCALS (SPSS, 1988) has been used (PRINCALS is an acronym for PRINCIPAL Components analysis by means of Alternating Least Squares).

In Fig. 6 an example of the PRINCALS-analysis is given. It is to be noted that it is a two dimensional representation of a three dimensional figure. In this plot the original measured variables are given. The angles between the vectors of the input variables are such that the whole plot is the best least squares representation of the correlations between all the variables. Vectors pointing in the same direction have a positive correlation, in opposite direction a negative one. The orientation of the variables with respect to the abscissa or "dimension 1" is such that the sum of the squares of the projections of the variables on this axis is maximized. In the process the variables are normalized

and one may say that this sum is the variance that is explained (or described) by dimension 1 (called eigenvalue for that dimension). The meaning of dimension 1 has to be identified by the investigator. In case of one variable only, the meaning of dimension 1 would be identical to that of the variable. In general the meaning of dimension 1 is to be found by recognizing the common aspects of the most important contributors. It is not necessarily a physical quantity, it might well be a quality or an identification of a process. In any case, dimension 1 is the first 'principal component' of all the information that is in the total set of data. The same accounts, *mutatis mutandis*, for the other axes. In this study three dimensions have been found necessary to describe the data.

Analyzing Fig. 6 shows that the process described by dimension 1 becomes more important in case the frequency ( $=FRQ$ ) and the stiffnesses  $S_m(0)$  ( $=M0$ ),  $S_m(N_i)$  ( $=MI$ ) and  $S_{m,rel}$  ( $=MR$ ) decrease and the temperature ( $=TMP$ ) and the life times  $N_i$  ( $=NI$ ),  $N_c$  ( $=NC$ ) and  $N_r$  ( $=NR$ ) increase. This is typical for bitumen, so bitumen must play the most important role in that part of the crack growth process represented by dimension 1. Referring to the phenotypes discussed before it is straightforward to ascribe this to phenotype 1: crack growth through the mortar. So dimension 1 is called "cohesive crack growth".

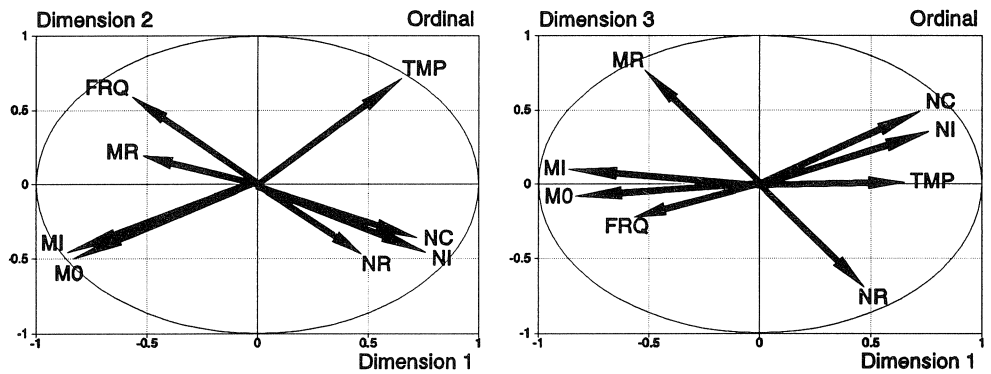


Fig. 6. A PRINCALS-plot, based on the crack foil measurements on SA.

In the same way it is found that dimension 2 in Fig. 6 describes in much lesser sense the bituminous aspects of a mix; also the non-bituminous ones seem to come into play. So dimension 2 is attributed to phenotype 2 and called adhesive crack growth (i.e. crack growth between the aggregate and the mortar). Dimension 3 depends essentially only on the relative stiffness and lifetime. This can be related to the third phenotype: crack growth retardation due to a change in direction of propagation, that might well occur in the neighbourhood of aggregates or air voids.

Of course, the total crack growth process may differ from mix to mix. In Table 2 the observed composition of the total crack growth is given for several mixes. The eigenvalues, which may be seen as the relative importance of the dimensions in the whole crack growth process, are given too.



Table 2. Principal processes recognized by PRINCALS-analysis (c.g.= crack growth; the numbers in brackets are the eigenvalues).

	Dimension 1	Dimension 2	Dimension 3
SA	cohesive c.g. (0.47)	adhesive c.g. (0.24)	retardant (0.19)
DAC8	adhesive c.g. (0.35)	cohesive c.g. (0.33)	retardant (0.14)
DAC16	cohesive c.g. (0.37)	retardant (0.20)	adhesive c.g. (0.19)
SMA	cohesive c.g. (0.41)	retardant (0.25)	adhesive c.g. (0.18)
All mixes	cohesive c.g. (0.43)	adhesive c.g. (0.28)	retardant (0.20)

So for all mixes, except DAC8, the cohesive crack growth process is the most important mechanism, as the eigenvalues show. For the DAC8 mix the eigenvalues for dimension 1 and dimension 2 are about equal, indicating that in this mix adhesive and cohesive crack growth determine the overall process. A similar remark goes for the dimensions 2 and 3 for the DAC16 mix.

The PRINCALS analyses indicate that the crack growth process in all tested mixes can be described with three principal processes (=dimensions). Comparison of eigenvalues shows that the first dimension of the SA mix corresponds with the second dimension of DAC8, the first of DAC16, the first of SMA and the first of AM (AM represents all available data). Thus the measured crack growth process in the involved AC mixes is constituted by three mechanisms. The differences between the mixes is the contribution of each of the mechanisms to the overall observed process.

## 4 The COD-measurements

COD-measurements indicate both the micro and macro crack growth process as it occurs in front of the gauges and can be used in the analysis using the Absolute Rate Theory (ART). Here rate stands for the change in time of a concentration of "molecular parts" in given energetic states. These states are called bonds. Such a bond can be in a "broken" or in a "non-broken" state. The time evolution of these states, and so of crack growth, is studied by ART.

In this paragraph first the size of the micro crack zone will be determined. After that the ART will be introduced briefly and then the COD-measurements will be used to determine the ART-parameters. More information about the ART and its application in the description of the crack growth process in AC mixes is given by Jacobs (1995).

### 4.1 The size of the micro crack zone

From Fig. 2 it is concluded that no simple relationship exists between the decrease of the force and the length of the macro crack, measured by the crack foil. This is ascribed to a micro crack zone which occurs in front of the macro crack (see Fig. 7). In this zone very small cracks develop which are not measured by the crack foil.

The size of the micro crack zone can be determined by comparing the crack foil and COD measurements. Broek (1991) has shown, based on fracture mechanics, that a linear relation exists between

the COD and the total damage zone (macro crack plus micro crack zone). This total damage zone is expressed as an equivalent crack length  $c_{eq}$ . The  $c_{eq}$  is the length of a single macro crack which yields the same COD-value as the existing macro crack and micro crack zone together.

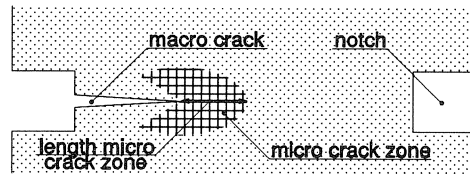


Fig. 7. The micro crack zone.

In the analyses presented here the following assumptions have been made:

- (a) the crack foil measurements determine by definition the damage in the specimen due to the macro crack,
- (b) the COD gauge measures the total damage in the material between the two notches,
- (c) the size of the micro crack zone is determined by the difference between the COD and the crack foil measurements.

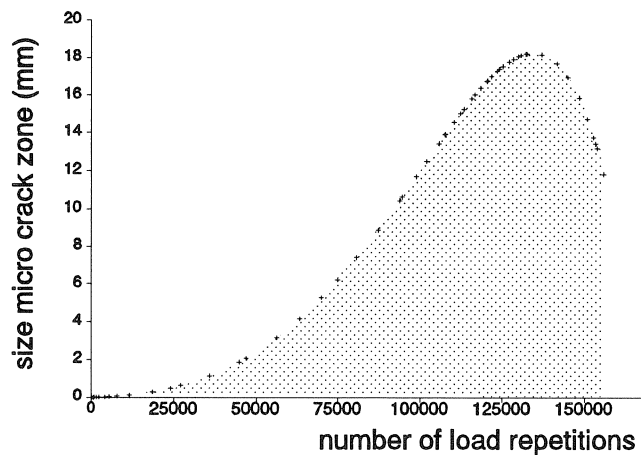


Fig. 8. An example of the size of the micro crack zone in a DAC16-specimen.

In Fig. 8 an example of the size of the micro crack zone is given. In this figure the size of the zone is given as a length. The following observations can be made:

- (a) immediately after the start of the test the micro crack zone starts to develop in the specimen,
- (b) during the dynamic test the micro crack zone and the macro crack grow until the micro crack zone contacts the other size of the specimen. From that point of time the size of the micro crack zone decreases,
- (c) at the end of the test the micro crack zone decreases quickly to zero because of the high macro crack growth velocity.

Based on the comparison of the size of the micro crack zone of specimens tested under identical loading situations, the following conclusions can be drawn:

- (1) for all tested specimens the micro crack zone achieves its maximum size at a relative number of load repetition ( $=N/N_c$ ) of  $0.92 \pm 0.04$ ,
- (2) the average size of the maximum relative micro crack zone, indicated hereafter between brackets, is the smallest for the SMA (0.57) and the DAC8 mix (0.59); the largest size occurs for the SA (0.68) and the DAC16 mix (0.69),
- (3) for all mixes it is found that the size of the micro crack zone increases with increasing temperature. This is caused by the fact that AC shows a more brittle behaviour at lower temperatures. Another reason is the fact that at higher temperatures larger deformation levels are applied in order to reduce the fatigue life of the specimens to about one hour ( $\approx 30000$  load repetitions). The influence of the deformation level is confirmed by measurement at various levels deformation levels at a constant temperature,
- (4) rest periods in the signal applied to the specimen decrease the size of the micro crack zone: the longer the rest periods, the smaller the micro zone. This is probably due to healing during the rest periods (Healing is the phenomenon in asphalt mixes and other viscous or fluid materials that a (micro) crack diminishes or even disappears if the material is left alone),
- (5) compaction, and by that the air voids, hardly influences the size of the micro crack zone, whereas an increase of the amount of bitumen and filler decreases its size. Using porphyry or granite instead of moraine aggregate also decreases the size of the zone, where the largest reduction occurs for the granite type of aggregate.

#### 4.2 *The Absolute Rate Theory*

ART was introduced in the 1920's to describe the plastic deformation of a material; Tobolsky and Eyring (1943) were the first who used the ART to describe the crack process in a polymer. After the introduction the theory has been used and extended by several researchers to describe cracking in various materials (from amorf to cristallic). Particularly the work of K ormeling (1986) on steel fibre reinforced concrete and van der Put (1989) on wood have contributed towards the development of the ART for non-linear composite and visco-elastic materials. Herrin and Jones (1963) and Herrin, Marek and Strauss (1966) were the first who used the ART to describe the deformation of bitumen under shear stress accounting for temperature. The results showed that the ART can potentially describe the behaviour of bitumen accurately.

In the ART emphasis is placed on processes on atomic and molecular level. The crack growth process can be described with the thermally and mechanically activated fracture process of primary bonds (e.g. covalent, metallic or ionic bonds) on atomic level and secondary bonds (e.g. van der Waals bonds) on molecular level. Although secondary bonds are weaker than primary bonds, they are strong enough to determine the final arrangement of groups of molecules in solids. They are important in the formation of the structures in asphaltic mixes. It is assumed that crack growth in AC mixes is related to breaking and forming of secondary bonds, which are randomly distributed over an area. Crack propagation is seen as a process in which the number of forward activated bonds (=bond breaking) is larger than the number of backward activated bonds (=bond forming), whereas the total number of involved bonds is constant. This means that in a crack growth process the

number of intact bonds will reduce until finally this number becomes zero and the material is completely fractured.

To achieve macro displacements, bonds have to be broken or deformed. Therefore an energy input, exceeding a certain minimum, is necessary. This energy level is the free activation energy  $Q_a$  of a bond. The value of this energy is typical for the involved process and material. Mechanical and thermal energy cooperate to reach this free activation energy. This is shown in Fig. 9: when bonds are moved from their equilibrium position by an external applied load, their potential energy is increased: the potential energy surface is changed from the solid to the balled line, making the reaction more probable by decreasing the relative height of the energy barrier  $Q_{a,f}$  with  $W_f$  for the forward direction and by increasing the barrier  $Q_{a,b}$  with  $w_b$  for the backward direction. It is mentioned that actual material behaviour is described by a number of parallel and/or sequential processes, each described by energy barriers shown in Fig. 9.

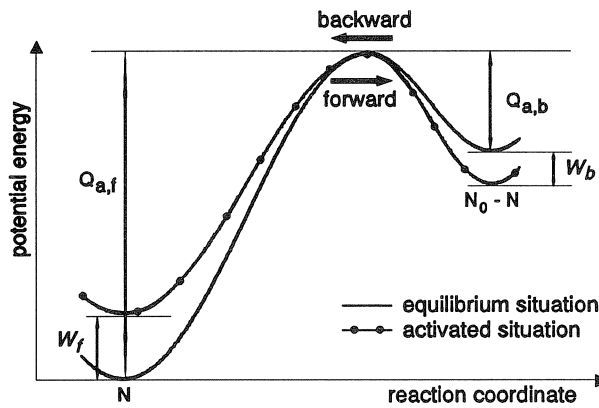


Fig. 9. The potential energy change for an elementary reaction along the reaction coordinate for a single energy barrier approach.

The total change in the material can be described by:

$$\begin{aligned}
 -\frac{dN}{dt} = & N \frac{kT}{h} \exp\left(-\frac{Q_{a,f}}{kT}\right) \exp\left(\frac{W_f}{NkT}\right) + \\
 & -(N_0 - N) \frac{kT}{h} \exp\left(-\frac{Q_{a,b}}{kT}\right) \exp\left(-\frac{W_b}{NkT}\right)
 \end{aligned}
 \tag{1}$$

where:

$h$  = Planck's constant =  $0.662618 \cdot 10^{-33}$  Js,

$Q_{a,f}$  = activation energy per bond in the forward direction (in J/bond),

$Q_{a,b}$  = activation energy per bond in the backward direction (in J/bond),

$W$  = total external applied energy (=work, in J),

- $W_f$  = external applied energy used in the forward reaction (in J),  
 $W_b$  = external applied energy used in the backward reaction (in J).  
 $N$  = number of bonds in the 'non-broken' state  
 $N_0$  = total number of available bonds

Equation (1) was first derived by Tobolsky and Eyring (1943). It was the starting point for researchers to describe deformation processes (creep, relaxation, fracture). In equation (1) the first term describes the forward (bond breaking) process while the second term characterizes the backward (bond forming) process.

#### 4.3 Determination of the ART parameters

In the interpretation according to ART, the following variables must be determined:

- The number of parallel and/or serial processes. In a serial approach various energy barriers in consecutive order must be passed through before breaking of a bond occurs; in a parallel approach various energy barriers occur simultaneously.
- The forward and backward energy terms.
- The forward and backward free activation energy.

As input the COD measurements provide a good and direct way to indicate the crack growth process. In order to prove that the COD-gauges mainly measure crack growth and hardly plastic deformation, fracture mechanics is used. The solution of the ART-equation is written in terms of the relative number of bonds per area  $N/N_0$  (see equation (5)). Because of consistency between the ratio  $N/N_0$  and the damage, the COD-data obtained for each individual specimen must also be formulated in relative terms:

$$\text{COD}_{\text{rel}} = \frac{N}{N_0} \quad (2)$$

using:

$$\text{COD}_{\text{rel}} = \frac{\text{COD}_{\text{max}} - \text{COD}}{\text{COD}_{\text{max}} - \text{COD}_{\text{min}}} \quad (3)$$

where:

- $\text{COD}$  = measured COD-value,  
 $\text{COD}_{\text{min}}$  = measured minimum COD-value,  
 $\text{COD}_{\text{max}}$  = measured maximum COD-value.

As stated before almost all fracture processes are complex combinations of many steps. It is one of the cardinal principles of the ART that the simplest possible model must be used to represent a process. For this reason a single barrier with bond breaking only should be adopted first as a model. If this proves insufficient, a single barrier with both breaking and forming rate constants provides the best candidate for the constitutive equation. If both models prove unsatisfactory, a multi-barrier mechanism must be considered.

To determine the ART-parameters graphically, one first has to reflect on the process under study. In the beginning of the fatigue test both the bond-breaking and bond-forming processes determine crack growth in a specimen. Then both processes are more or less in equilibrium: the macroscopic material properties do not change. During the cyclic test the intensity of the bond-breaking process increases with respect to that of the bond-forming process, causing crack growth in the specimen. At the end of the test, when the increase in crack length is fast, the bond-forming process is negligible to the bond-breaking process. This implies that for this last process the second term of the right part of equation (1) disappears, leaving a differential equation by which the  $Q_{a,f}$ -value and the ratio between  $W_i$  and  $N_0$  can be determined. So, using the definition of  $x$  in relationship 5, one obtains:

$$-\frac{dN}{dt} = N \frac{kT}{h} \exp\left(-\frac{Q_{a,f}}{kT}\right) \exp\left(\frac{W_f}{NkT}\right) \quad (4)$$

$$x = \frac{N}{N_0} \quad (5)$$

$$-\frac{dx}{dt} = x \frac{kT}{h} \exp\left(-\frac{Q_{a,f}}{kT}\right) \exp\left(\frac{W_f}{xN_0kT}\right) \quad (6)$$

$$\begin{aligned} \ln\left(-\frac{1}{x} \frac{\Delta x}{\Delta t}\right) &= \ln\left[\frac{kT}{h} \exp\left(-\frac{Q_{a,f}}{kT}\right)\right] + \frac{1}{x} \frac{W_f}{N_0kT} \\ &= a + \frac{1}{x}b \end{aligned} \quad (7)$$

Here the increment ( $\Delta$ ) is used for differential notation. From the intersection (a) of the straight line with the vertical, the value of  $Q_{a,f}$  can be determined; from the slope the ratio  $W_i/N_0$ .

In Fig. 10 an example of the graphical analysis for the last part of the actual crack growth process is given according to relationship (7). For the DAC8, DAC16, DACmod and SMA three parallel processes are necessary, for the SA mix it is found that two parallel processes suffice to describe this part of the fracture process. Again using PRINCALS-analysis it is found again that these three processes are the cohesive and adhesive crack growth process and the crack arrestors. So these three processes are identical to the three processes that were found with the analysis of the crack foil measurements. So with different theoretical approaches and different crack growth measurements the same three processes have been recognised in the crack propagation phase in AC mixes. Further analysis showed that the slopes of the parallel processes are approximately equal, indicating that the ratio's  $W_i/N_0$  for the three parallel forward reactions are equal.

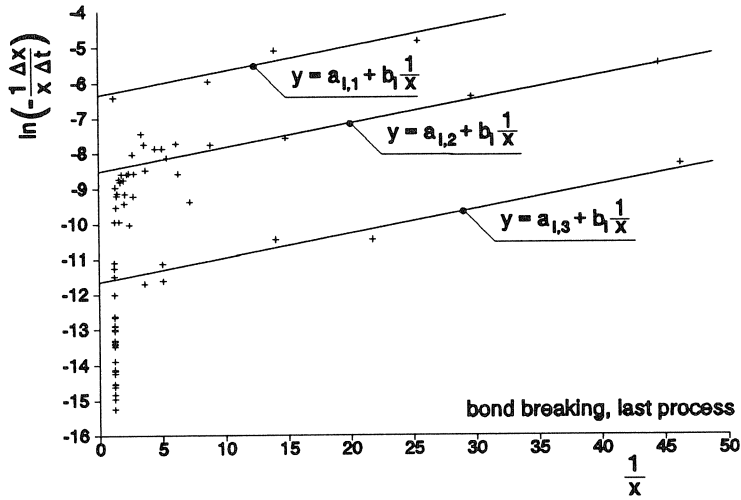


Fig. 10. Graphical determination of forward ART-parameters in the last part of the crack growth process assuming three parallel processes for specimen DAC16\_123.

After determination of the parallel forward processes, the backward parts can be determined by subtracting the first determined forward process from the original data set. On the resulting data the same procedure is used as for the determination of the parameters of the forward process.

Rewriting:

$$A = \frac{kT}{h}; B = \exp\left(-\frac{Q_{a,f}^*}{kT}\right); C = \exp\left(-\frac{Q_{a,b}}{kT}\right) \quad (8)$$

relationship (1) can be written as:

$$\frac{dx}{dt} = xAB \exp\left(\frac{1}{xkT} \frac{W_f^*}{N_0}\right) - (1-x)AC \exp\left(-\frac{1}{xkT} \frac{W_b}{N_0}\right) \quad (9)$$

where:

$W_f^*$  = graphically determined energy for the forward process,

$Q_{a,f}^*$  = graphically determined free activation energy for the forward process.

Both  $W_f^*$  and  $Q_{a,f}^*$  consist of three (for SA two) terms because of the three parallel processes.

Reformulating equation (9) results in:

$$\begin{aligned} \ln \left[ \frac{1}{1-x} \frac{\Delta x}{\Delta t} + \frac{x}{1-x} AB \exp\left(\frac{1}{xkT} \frac{W_f^*}{N_0}\right) \right] &= \\ = \ln(AC) - \frac{1}{x} \frac{W_b}{N_0 kT} &= m - \frac{1}{x} n \end{aligned} \quad (10)$$

where:

$$Q_{a,b} = -kT \left[ m + \ln \left( \frac{h}{kT} \right) \right]; \frac{W_b}{N_0} = nkT \quad (11)$$

The graphical determination of the backward processes show that only one backward process can be recognised. Probably this is the cohesive crack growth process (the bonds in the mortar), because in this process most of the low molecular weight parts (the so called maltenes) are involved which diffuse easily and so may be able to rebind relative easily. Here it is assumed implicitly that the bonds associated with the adhesive crack growth and crack stoppers do not recover (bond forming is much smaller as for the cohesive crack growth process).

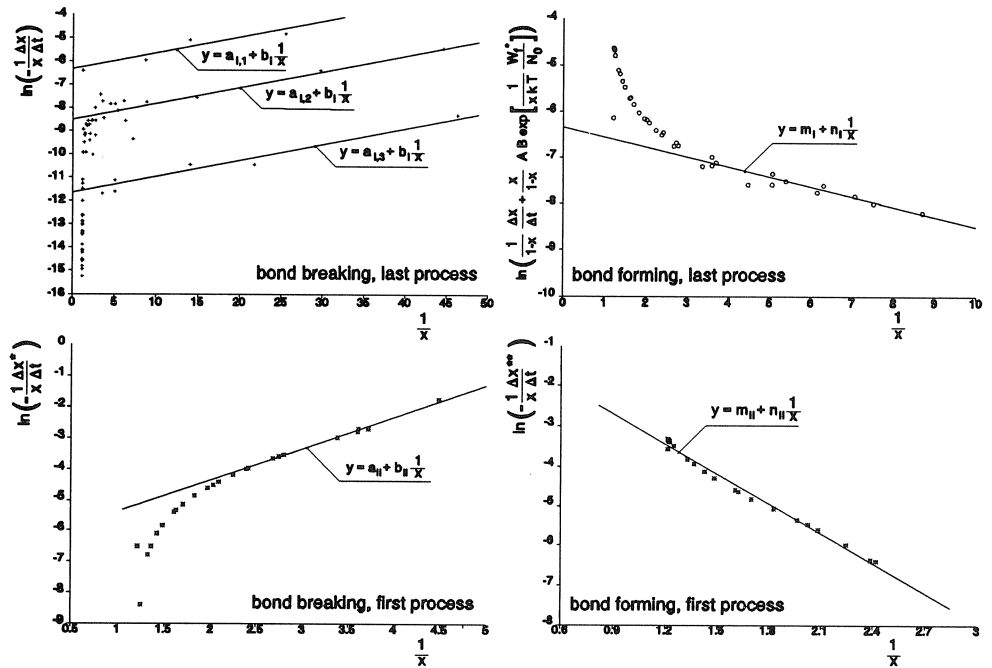


Fig. 11. Overview of the graphical determination of the ART-parameters in specimen DAC16\_123.

So now all ART-parameters for the last phase in the actual crack growth are determined. Now the following part, which actually precedes the analyzed part, can be analyzed. An overview of the graphical determination of all parameters in all processes is given in Fig. 11. It appears that the first part of the actual crack growth (under analysis now) can be described with one forward and one backward process. As the data points of the backward process are approximately on a straight line, one may conclude that no further processes are involved in the actual crack growth process. This means that the complete crack growth process can be characterised by Fig. 12.



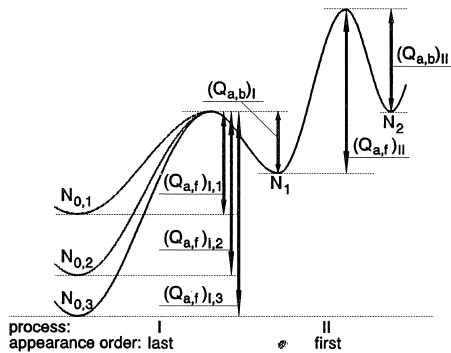


Fig. 12. Description of the crack growth process with the ART-approach using three parallel processes.

The assumed three parallel processes in the last part of the crack growth process are distinguished in all specimens except for the SA mix where only two are recognised. In SA specimens the adhesive crack growth process is missing. This is reasonable because due to the absence of larger aggregate parts in the SA mix, the complete crack growth must occur in the mortar (which takes the least amount of energy).

Comparison of the ART parameters of both backward processes (in terms of the ratio's  $W_{b,i}/Q_{b,i}$ ) indicates that bond forming in the first (actual) process is much more important than in the second (last occurring) process. In case bond forming is associated with healing (as mentioned before: it is a phenomenon which lengthens the life time by a factor 4–6) this implies that the largest part of the healing process occurs during the first process in the crack initiation phase.

From these analyses it is concluded that parallel and serial processes in the ART description of crack growth in AC mixes is in agreement with the physics behind it.

## 5 Conclusions

From the experimental results, the analyzed data and the theoretical approach presented in this paper, the following conclusions can be drawn:

- Crack growth in AC mixes can be described by a process in which macro cracks are preceded by micro crack zones. The macro cracks in asphaltic mixes grow discontinuously; the discontinuity increases with increasing aggregate size.
- Crack growth measurements in AC mixes using crack foils at the outside of the specimens indicate that the fracture process consists of three parallel occurring processes: cohesive crack growth through the mortar, adhesive crack growth separating the aggregate from the mortar and a crack retardant process. This last process is a temporary decrease in crack growth speed caused by a change in crack growth direction due to aggregates or air voids. The differences in crack growth characteristics between AC mixes is due to different contributions of each process to the overall behaviour.

- (c) Analyzing the measured fracture damage (by COD gauges) with the ART indicates that the crack initiation phase can be described with one bond forming and one bond breaking process, whereas the crack propagation phase is described by three parallel processes: a cohesive crack growth, an adhesive crack growth and a crack retardant process.

## Notations

$h$	Planck's constant = $0.662618 \cdot 10^{-33}$ Js
$k$	Boltzmann constant = $13.8066 \cdot 10^{-24}$ J/K
$N$	the number of intact bonds per unit area
$N_0$	total number of relevant bonds in the virgin material at $t = 0$ s per unit area
$N_i$	the number of load repetitions at which crack initiation occurs
$N_c$	the number of load repetitions until collapse of the specimen
$N_{rel}$	ratio between $N_i$ and $N_c$
$Q_{a,f}$	activation energy per bond in the forward direction
$Q_{a,b}$	activation energy per bond in the backward direction
$S_m(0)$	the corrected initial stiffness
$S_m(N_i)$	the stiffness modulus at crack initiation
$S_{m,rel}$	the ratio between $S_m(0)$ and $S_m(N_i)$
$T$	the absolute temperature
$W$	total external applied energy (=work)
$W_f$	external applied energy used in the forward reaction
$W_b$	external applied energy used in the backward reaction

## References

- BROEK, D. (1991), *Elementary Engineering Fracture Mechanics*, Kluwer Academic Publishers, Dordrecht, The Netherlands.
- HERRIN, M. and JONES, G.E. (1963), The Behaviour of Bituminous Materials from the Viewpoint of the Absolute Rate Theory, In *Proceedings Association of Asphalt Paving Technologists*, Vol. 32, pp.82–105.
- HERRIN, M., MAREK, C.R. and STRAUSS, R. (1966), The Application of the Absolute Rate Theory in Explaining the Behaviour of Bituminous Materials, In *Proceedings Association of Asphalt Paving Technologists*, Vol.35, pp.1–18.
- HOPMAN, P.C., KUNST, P.A.J.C. and PRONK, A.C. (1989), A Renewed Interpretation Method for Fatigue Measurements: Verification of Miner's Rule, In *Proceedings Eurobitume Conference*, Vol.1, Madrid, pp.556–561.
- HORDIJK, D.A. and REINHARDT, H.W. (1989), Macro-structural Effects in a Uniaxial Tensile Test on Concrete, In: *Brittle Matrix Composites – 2* (Eds. Brandt, A.M. and Marshall, I.H.), Elsevier Applied Science, pp.486–495.

- JACOBS, M.M.J. (1995), Crack Growth in Asphaltic Mixes, *Ph.D.-Dissertation*, Delft University of Technology, Road and Railroad Research Laboratory, ISBN 90-9007965-3.
- KÖRMELING, H.A. (1986), Strain Rate and Temperature Behaviour of Steel Fibre Concrete in Tension, *PhD-Dissertation*, Faculty of Civil Engineering, Delft University of Technology.
- KRAUSZ, A.S. and EYRING, H. (1975), Deformation Kinetics, *A Wiley Interscience Publication*, ISBN 0-471-24983-1.
- VAN DER PUT, T.A.C.M. (1989), Deformation and Damage Processes in Wood, *PhD-Dissertation*, Faculty of Civil Engineering, Delft University of Technology.
- SPSS (1988), Statistical Package for Social Science SPSS/PC, SPSS/PC+Advanced Statistics V2.0, SPSS Europe B.V., Gorinchem, The Netherlands.
- TOBOLSKY, A. and EYRING, H. (1943), Mechanical Properties of Polymeric Materials, In *Journal of Chemical Physics*, Vol. 11.

